Filipa Rodrigues Filipe Fernandes

Bachelor in Micro and Nanotechnology Engineering

Development of an Ignition Coil Integrated System to Monitor the Spark Plugs Wear

Dissertation submitted in partial fulfilment
of the requirements for the degree of

Master of Science in
Micro and Nanotechnologies Engineering

Adviser:	Dipl.-Ing. (FH) Marco Lönarz, Product Development Engineer, Delphi Powertrain Systems, Luxembourg
Co-advisers:	Dr.-Ing. Peter Weyand, Engineering Manager Ignition Europe, Delphi Powertrain Systems, Luxembourg
	Pedro Miguel Cândido Barquinha, Assistant Professor, Faculty of Sciences and Technology, NOVA University of Lisbon

Examination Commitee

Commitee Chair:	Dr. Rodrigo Ferrão de Paiva Martins, Full Professor, Faculty of Sciences and Technology, NOVA University of Lisbon
Raporteur:	Dipl.-Ing (FH) Marco Lönarz, Development Engineer, Delphi Powertrain Systems, Luxembourg
Examiner:	Telmo Jorge Gomes dos Santos, Assistant Professor, Faculty of Sciences and Technology, NOVA University of Lisbon

FACULDADE DE
CIÊNCIAS E TECNOLOGIA
UNIVERSIDADE NOVA DE LISBOA

October, 2016

Aos importantes que não deixaram de o ser na "ocidental praia lusitana" e aos
que em tal se tornaram no "Eldorado"

Acknowledgements

who didn't forget to be my best friends, even when we didn´t talk for months but we felt like we did. To all these people, thank you so much for your "goodbye" and "welcome home" hugs and for making me miss Portugal until the day I came back.

And finally, to my greatest support throughout this whole time, by being there for me any time of any day, to tell and to listen to the stupid, crazy and serious stuff, I have to dedicate this thesis to you David, because, except for the technical part, you know all about it (and you could even help me in the technical part!). All the photos, the future plans, the HTGAWM and House of Cards episodes, the "Desculpa, tenho de ir correr" moments, the company in car trips and in the shower, the breaks during calls on all types of platforms, the "Hoje, íamos passear ali" wishes, the company during that couple of days at home with a stiff neck and all the one-sentence letters to put on the wall are just the trailer of what we are and what we became together. So a big thank you and I look forward for the time I can be there for you as much as you were for me.

Abstract

Automotive industry is undergoing significant changes to answer new emission limits and cost restrictions. These lead to unfavourable operating conditions for the components (including spark plugs and ignition coils): overheating, higher pressures, downsizing and leaner air/fuel mixtures.

Consequently, the ignition coil integrated system is being asked for stronger and multiple sparks and longer burning times. In response, rare precious metals (iridium, platinum, tungsten) must be utilized, resulting in a cost increase thereof. Hence, it is a main interest to monitor these high quality components.

In this work, Paschen Law is used to find a relation between the electrodes gap (ultimately related to wear conditions) and breakdown voltage. Thereby, this thesis is mainly focused on developing a method to monitor the referred voltage. In a transistorized coil ignition (TCI) system, the microcontroller can measure a time which is directly proportional to the breakdown voltage. That information is collected coil-internally and communicated to the ECU. The latter carries out statistical data analysis along with real-time pressure, load and speed data.

After laboratory and car tests, it was proved that the secondary current sensing circuit may also serve as a breakdown voltage sensor, eliminating the need for any cost increase rather than development costs concerning mass production of ignition coils.

Keywords: Spark plugs, Ignition Coil, Paschen Law, Electrodes Gap, Wear, Breakdown Voltage, TCI, Microcnotroller, ECU, Pressure, Load

Resumo

A indústria automóvel atravessa uma fase de mudança em respondsta a novos limites de emissões e restrições de custo, o que resulta em condições desfavoráveis para os componentes (incluindo velas de ignição e ignições): sobreaquecimento, pressões altas, miniaturização e misturas de ar/combustível mais pobres.

O sistema integrado de ignição é forçado a providenciar faíscas mais fortes e múltiplas e combustões mais longas. Para compensar, utilizam-se metais preciosos raros (irídio, platina, tungsténio), aumentando o custo dos componentes. É, portanto, de grande interesse monitorizar estes componentes de alta gama.

Através da Lei de Paschen, estabelece-se a ligação entre a distância entre eléctrodos (relacionada com as condições de desgaste das velas) e a tensão de rutura. Como tal, esta tese é maioritariamente focada no desenvolvimento de um método de monitorização dessa tensão. Num sistema TCI (*Transistorized Coil Ignition*) o microcontrolador mede um intervalo de tempo diretamente proporcional à tensão de rutura. A ignição recolhe essa informação, transmitindo-a à ECU, que procede a uma análise estatística, em conjunto com valores de pressão, carga e velocidade em tempo real.

Testes em laboratório e num carro provaram que o circuito sensor de corrente do fio secundário da bobine serve igualmente de sensor da tensão de rutura, não havendo qualquer aumento de custo além do custo de desenvolvimento aquando da produção em massa de ignições.

Palavras-chave: Velas de Ignição, Ignições, Lei de Paschen, Distância entre Elétrodos, Desgaste, Tensão de Rutura, Microcontrolador, TCI, ECU, Pressão, Carga

List of Abbreviations

ADC – Analog to Digital Converter

ALU – Arithmetic Logic Unit

BDC – Bottom Dead Centre

CNG – Compressed Natural Gas

ECU – Engine Control Unit

EGR – Exhaust Gas Recirculation

EST – Electronic Spark Timing

IGBT – Insulated Gate Bipolar Transistor

PCB – Printed Circuit Board

PWM – Pulse-Width Modulation

TCI – Transistorized Coil Ignition

TDC – Top Dead Centre

List of Symbols

bar – Bar (unit of pressure)

CO_2 – Carbon dioxide

C_{Load} – Load capacitance

C_S – Capacitance of the secondary winding

d – Distance between two electrodes (electrodes gap)

D_S – Diode of the secondary winding

F – Farad (unit of capacitance)

g – Gram (unit of mass)

Hz – Hertz (unit of frequency)

I_P – Current in the primary winding (primary current)

I_{P_Th} – Primary Current Threshold

I_S – Current in the secondary winding (secondary current)

K – Kelvin (unit of temperature)

ln – Natural Logarithm

L_P – Inductivity of the primary winding

m – Metre (unit of length)

°C – Degree Celsius (unit of temperature)

p – Pressure

Pa – Pascal (unit of pressure)

Q_1 – Switch embodied by an IGBT

R_P – Resistance of the primary winding

R_S – Resistance of the secondary winding

s – Second (unit of time)

t_B – Breakdown timing

t_{IGBT} – Moment when the IGBT is disconnected from ground

t_{Is} – Moment when I_S drops below Vth(I_S)

t_{OUT} – Maximum time the microcontroller seeks for t_{Is} and t_B

ü – Turns ratio

U_b – Supply voltage

v – Velocity

V – Volt (unit of electric potential)

V_B – Breakdown voltage

$V_{B,crit}$ – Critical value of V_B

V_{C-} – Collector voltage

V_{dd} – Drain voltage

V_{Is} – Voltage across the secondary current shunt resistor at t_B

$V_{th}(I_S)$ – Threshold of the voltage across the secondary current resistor

Z_S – Impedance of the spark plug

γ – Secondary emission coefficient

Table of Contents

List of Tables

List of Figures

Motivation and Objectives

Motivation

Horizon 2020 is a long-term programme, set by European Union, which aims to a customer-driven technology and innovation leadership by funding R&D in public and private sectors as well as developing European policies accordingly, [1]. In the wake of this comprehensive program, and more specifically of European Union's Regulation (EC) No 443/2009, there has been a cumulative effort to achieve the average consumption target of 95g CO_2/km set for the newly registered fleet, phased in from 2020. [2], [3] Although for some, as *B. Geringer*, the aforementioned value might not serve as a strict limit, but a benchmark instead, the automotive industry is already coming up with innovative solutions at the engine level such as downsizing of Otto-engines, Lean Burn Processes (usage of mixtures inside the cylinder with a high air/fuel ratio), Stratified Combustion and High Dilution Exhaust Gas Recirculation (EGR). [3], [4] With these combustion processes, however, a diversity of drawbacks related to boundary conditions comes along. For that same reason, Horizon 2020 has been a driving force likewise for development of injection and ignition systems which can compensate for some of those shortcomings. [4]

The effects of spark ignition regarding combustion and engine performance and vice-versa have been a subject of many researches. [5] Nevertheless, it is known that the latest developments in the automotive industry, especially in response to emission limits and cost reduction, have imposed unfavourable conditions to the components, such as overheating, higher pressures, downsizing and poorer air/fuel mixtures which must be overcome through design changes and the usage of new materials. [4], [6] The ignition coil integrated system is an example of such evolution. Leaner air/fuel mixtures, exhaust emission controls and suchlike goals require stronger and/or multiple sparks and longer burning times. [3], [4], [7] This, in turn, leads to severe wear of spark plug electrodes, besides the inevitable damage these materials undergo due to extreme pressures and temperatures generated during the normal ignition process inside the combustion chamber. [5], [6] Thereby, one can observe an increasing trend to use precious metals, namely iridium, platinum and tungsten, which significantly increase manufacturing costs. [5] Consequently, there is a crescent interest in monitoring this type of modern

spark plugs. The ultimate consequence of using a worn out spark plug is misfire, *i.e.* the air/fuel mixture is not ignited inside the combustion chamber, which leads to discomfort for the driver as well as increase of CO_2 emissions. [8]

Digital electronics have been doubtless playing a major role in instrumentation and control for automotive technology, in which the engine system is one of the most significant control applications. Low cost and real-time adaptability are the leading advantages of utilizing a microprocessor-based engine control system. [9] An engine control unit (ECU) of this sort opens doors to the implementation of new coil-internal features by the usage of a microcontroller implying minimal or even any change to the peripheral circuitry but software improvements instead.

Objectives

It is a main goal of the present work to investigate a possible solution to monitor spark plugs wear through the measurement of breakdown voltage. Plainly put, the primary objective consists in measuring the breakdown voltage through the ignition coil integrated system, more precisely, making use of the microcontroller flexibility and available memory. In order to fulfil these objectives, the thesis was divided into five main steps:

- Getting familiar with the ignition coil integrated system
- Understanding its role in the engine working principle
- Studying the parameters that influence the breakdown voltage and its measurement
- Establishing a correlation between breakdown voltage and spark plugs wear conditions
- Propose a method of detection and monitoring thereof

Finally, some considerations must be made regarding future challenges and developments, calling for further work on this issue.

1   Introduction

1.1 Ignition Phenomena inside the Combustion Engine

This work will focus on four-cylinder four-stroke internal combustion engines, for which the ignition system used corresponds to. This kind of engine is a heat engine because it transforms thermal energy from chemical reactions into mechanical work. It is also an internal combustion engine, *i.e.* the products of combustion form the working fluid. Since combustion is initiated by a spark, it is named a spark-ignition engine. [10] Figure 1.1 embodies one of four in-line sets that compound a four-cylinder gasoline engine. The respective cycle of operation – Otto cycle – is presented. Its name was given after Nikolaus Otto who built, in 1876, the first engine embodying such principle. [11]
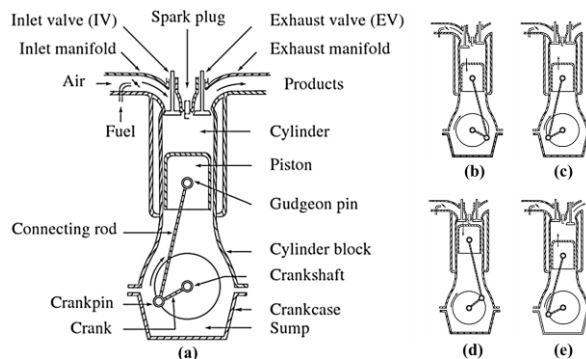
Figure 1.1: (a) Cross-sectional view of a spark ignition engine; Otto cycle: (b) intake, (c) compression, (d) expansion and (e) exhaust strokes. Adapted from [10]

During intake stroke, the piston is at the Top Dead Centre, TDC, (topmost position of the cylinder, where $v = 0$ m/s) and only inlet valve is open. [10] The motion of the piston downwards draws the air/fuel mixture into the combustion chamber (variable volume between cylinder head and the top of the piston at each moment). [10], [12] When the latter reaches Bottom Dead Centre, BDC, (the closest position to the crankshaft) the intake valve is closed and the stroke is finished. The mixture inside the combustion chamber is then compressed by an upwards motion of the piston, while both valves are closed. Close to the finish of second stroke, ignition system provides the necessary voltage to ignite the working fluid. Once the piston reaches TDC, combustion is initiated by a spark plug which provides an electric discharge and a flame kernel is established. Therefrom, chemical energy from the fuel is converted into heat energy dur-

ing the burning of the mixture, causing temperature and pressure to rise. The aforementioned pressure is then responsible for pushing the piston back to BDC and the flame kernel turns into a self-sustaining and expanding flame front. Expansion stroke has the duration of this downwards motion and power is only obtained during this time. [10] Expansion is finished when the exhaust valve opens. Henceforth, during exhaust stroke, the piston moves towards TDC, forcing the burnt gases to be purged from the cylinder. [12] The exhaust gases trapped in the cylinder after last stroke (residual gases), along with fresh charge, make the working fluid for the following cycle. [10], [12]

1.2 Ignition Coil Integrated System

It is a main function of the ignition coil integrated system to ignite the air/fuel mixture inside the combustion chamber– over the full speed and load range – at a precise moment, as well as undertake pre-determined safety features. [8], [10] Recently, there were added diagnostics features such as those to detect misfire or engine knocking. [8] The ignition system must be light, compact, reliable and low cost. [10]

Regarding gasoline engines, inductive high voltage generation (a spark ignition system) is currently the dominant process to initiate and sustain ignition phenomena, having surpassed capacitive high voltage generation. [8] Alternative technologies differ on spark plug type and/or phenomenon that leads to ignition. Such embodiments can either be spark ignition systems (e.g. MultiCharge, *i.e.* an ignition system providing multiple sparks per Otto cycle) or spatial ignition systems (e.g. corona, laser and microwave ignitions). [3], [4] The last category entails complex modifications in the engine and the spark plug, thus the associated costs hinder a suitable business case for passenger cars. [4] This work is based on inductive ignition, specifically on Transistor Coil Ignition, hence the subsequent descriptions will focus on such. [10]

1.2.1 The Spark Plug

The embodiment in Figure 1.2 describes the generic composition of a spark plug.
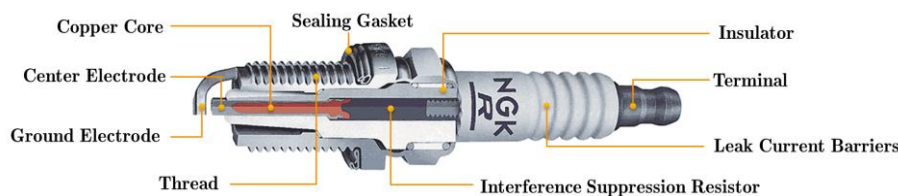
Figure 1.2: Sectional view of the generic composition of a spark plug. Adapted from [13]

The spark plug is composed of three main parts: shell, insulator and electrodes. The first one supports the ceramic insulator and its threads screw into the combustion

chamber spark plug hole, wherein the gasket is the sealing element. [12] The insulator generally consists of refractory high alumina sealed inside the shell, making a thermal and pressure seal. [12], [14] This component must withstand high thermal and pressure fluctuations as well as mechanical stress while preventing leakage and restricting the spark to the spark plug gap. Consequently, it is requested that the insulator material presents high thermal conductivity, electrical resistance and mechanical strength. [12] The insulator has a center bore in which the center electrode with a copper core is located. [14] Ground electrode, in turn, is connected to the shell and the distance between both electrodes is named spark plug gap or electrodes gap. Also in the center bore, it is possible to find a built-in resistor to limit the interference to TV and radio receivers. [12]

The high voltage generated by the ignition coil creates a voltage gradient within the electrodes gap capable of ionizing the air/fuel mixture therein. Therefore, a flame kernel is created and the combustion initiated. [10], [12]

Electrodes Wear

Spark plug tips are optimized to work between 400 °C and 850 °C. Below this range, the temperature is insufficient to evaporate carbon, metallic oxides and oil deposits on the insulator tip during consecutive cycles. [12], [15] This coating is electrically conductive and might short-circuit the spark plug, leading to misfire. [12] If the spark plug runs above 850 °C, erosion becomes more relevant, the insulator may become damaged and the air/fuel mixture is more prone to pre-ignition. [12], [15] In both situations, the electrodes present a non-uniform wear thus gap growth is also heterogeneous. For full load conditions and high rpm in a gasoline engine, center electrode is generally hotter than ground electrode (the temperature difference depending on load and frequency of rotation, rpm). This increases the erosion rate on the center electrode. [15]

The material and geometry of these electrodes has been changing towards smaller diameters and materials like Iridium, Platinum and Tungsten in order to reduce the requested breakdown voltage as well as the erosion caused by the required high currents in the spark plug electrodes. [5], [9], [12]

1.2.2 Ignition Spark Phases

It was proposed a division of the spark generation into four phases by Rudolf Maly in 1984. [9] These were named Pre-breakdown Phase, Breakdown Phase, Arc Discharge and ultimately Glow Discharge. [9], [16]

Pre-breakdown phase extends for a few microseconds and is characterized by an increasing electric field between the spark plug electrodes. During breakdown phase (in nanoseconds range), a self-created space charge is concentrated in a narrow channel be-

tween the electrodes wherein a partial volume has higher conductivity allowing for a higher current flux to be carried out. [9] The temperatures consequently increase in the range of 50000 K to 60000 K. [16] This step of the ignition event is the most relevant for the combustion process. [5] Following the Breakdown Phase, high current arc discharge arises, lasting for a few microseconds. [5], [9] During the referred interval, when comparing to breakdown phase, there is a drop of plasma temperature (5000K to 6000K). [16] For this arc to be sustained, electrons must be emitted from the cathode surface, specifically from pools of molten material named hot cathode spots. [9] These are the outcome of high current densities at the electrodes. The drawback of this mandatory event is the significant damage of the electrode surface, therefore this discharge phase is the most critical regarding the wear of the spark plug electrodes. [5], [9], [16] It is possible to define a transition period wherein one can observe a frequent commutation from arc to glow discharges and vice-versa. Arc discharge arises whenever a strong electric field and/or high pressure occur in the electrodes gap therefrom establishing high current densities in the cathode. [16] The major distinction between arc and glow discharges is the cold cathode of the last, since feedback electrons are generated by ion impact, thereby it is desired a rapid transition to low current glow discharge in order to minimize the electrode wear (essentially caused by sputtering throughout burning time). [9], [16] Usually, glow discharge extends for several milliseconds. [9]

1.3 Breakdown Voltage Detection

The voltage established in the electrodes gap which is necessary to ignite the air/fuel mixture – hereinafter referred to as breakdown voltage, V_B – depends on the following parameters (not listed by order of relevance): air/fuel ratio, fuel type, geometry of the electrodes, pressure within the electrodes gap, width of the aforementioned gap, electrodes temperature and surface conditions, fouling of insulator tip, internal impedance of the spark plug and voltage increase rate provided by the ignition coil. [5], [12]

For example, the required V_B is higher for lean mixtures, since the greater the air fraction present in the mixture, the lower is the electrical conductivity thereof. For the same reason, fuels that demand high air/fuel ratio call for higher V_B (e.g. compressed natural gas, CNG, compared to gasoline). [5] The electrodes shape play an important role in determining V_B as downsizing of both the centre and the ground electrodes allows for a higher strength of the electrical field therein, thus leading to a decrease of the required breakdown voltage. However, this energy concentration on the electrode tip must not reach such level that is generating a critical temperature on the electrode tip. In such circumstances, the electrodes erosion builds up and the spark plug lifetime is

shortened. [5] High pressures (result of load conditions in the car, which varies with driving conditions), on the other hand, entail as well higher voltages, because it means that a greater density of molecules is present in the spark plug gap, *i.e.* the mean free path decreases, thus the electrons must have a greater acceleration in order to ionize those same molecules. [5], [7] Otherwise, a conductive streamer is not established in the spark gap and the arc does not occur. A wider spark plug gap implies as well a greater V_B, since the energy has to be sufficient to ionize more widely spaced fuel molecules which are then combined with air molecules to start an exothermic reaction. In this case, the energy also has to be enough to sustain the flame kernel up to a suitable temperature and compensate for the unusable collisions between electrons and air molecules. The spark plug gap, however, is enlarged over time due to erosion that takes place during discharge. Simultaneously, the deposits on the insulator tip or a low voltage build-up rate reduce the voltage impressed in the electrodes gap, demanding a higher V_B. [12] Notwithstanding, the supply voltage of the ignition coil has a limit. If gap growth brings about a breakdown voltage above this limit, misfire events can arise, potentially causing damage to the catalytic converter and discomfort to the driver. [5] During driving, speed and load conditions vary continuously. It is known that both of them lead to an increase of the V_B. However, the quantification of this influence is yet to be determined in the scope of this work.

1.3.1 Paschen Law

It was in 1889 that Friedrich Paschen established the relation between breakdown voltage, pressure and spark plug gap. [17] Paschen Law can be translated in Equation 1,

$$V_B = B \frac{pd}{\ln(Apd) - \ln\left(\ln\left(1 + \gamma^{-1}\right)\right)} \tag{1}$$

where V_B is the breakdown voltage, p and d represent the pressure and width of the spark plug gap, respectively, γ is the secondary emission coefficient (or second Townsend coefficient) and A and B are constants that depend on the mixture of air and fuel between the electrodes. [18], [19] It is possible to ascertain that the required V_B is lower for a smaller gap. Nonetheless, reducing the spark plug gap might bring on a decrease in the plug performance when dealing with mixtures with high air/fuel ratios, unless this limitation is considered in the electrodes design, because there is a lower amount of fuel molecules in the electrodes gap. [5] Equation 1 results in the Paschen Curve (Figure 1.3).
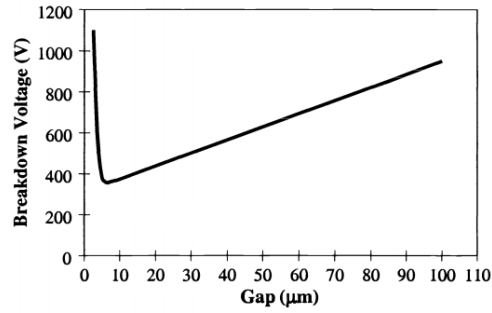
Figure 1.3: Paschen curve for air: gaseous breakdown voltage as a function of the distance between two conductors, at 1 atm. Adapted from [20]

Paschen curve depends on the gas in which the breakdown occurs and electrodes material, although the latter has less influence. [18] Paschen Curve enables the study of the gap through V_B measurements. Therefrom, it is theoretically possible to infer wear conditions of the plug electrodes. The hardship of this analysis mainly consists in isolating other wear sources that might affect V_B (for instance, when comparing two spark plugs with equal electrodes gap, the voltage is usually higher for the fouled plug). [5]

2 Materials and Methods

The monitoring system disclosured in the present work was developed for a transistorized coil ignition system (TCI) model and all the used setups were assembled according to such ignition embodiment.

2.1 Transistorized Coil Ignition System

TCI systems provide a higher secondary voltage and are characterized by a lower wear of its components, which demands a reduced maintenance and provides a higher reliability, even in the presence of lean mixtures. [8] Consequently, the spark plug lifetime is extended. TCI is currently the most common ignition system for gasoline engines due to its comparably low cost. [7]
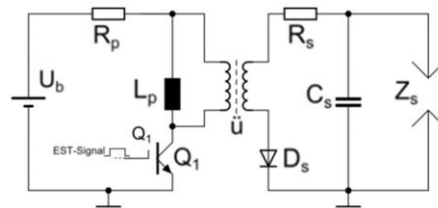
Figure 2.1: Simplified schematic of a standard TCI system. [7]

Firstly, it consists in a selectively controllable step-up transformer with turns ratio $ü$, *i.e.* a low voltage is established in the primary winding originating a high voltage in the secondary winding due to a selective storage and transference of energy. [21] While a supply voltage, U_b, (provided, in this case, by the vehicle battery) is fed into the first end of the foregoing primary winding, the opposite end is connected to a switch, Q_1. In the considered setup, the latter is embodied solely as an IGBT (Insulated Gate Bipolar Transistor), even though it may be coupled to additional components. Secondary winding, in turn, has one of its ends – the low voltage side – connected to ground through circuitry and the other one – the high voltage side – to the spark plug. R_P and L_P represent the primary winding resistance and inductivity while R_S and C_S represent secondary winding resistance and capacitance, respectively. There is also a control circuit that includes, for the embodiment considered, a microcontroller, which working principle will be explained after Figure 2.2. The referred control circuit provides an ignition control

voltage signal, responsible for periodically grounding the IGBT and thereupon causing an electrical current to flow through the primary winding and energy to be stored therein. If the transistor is then disconnected from ground, primary current is ceased, the stored energy is transferred to the secondary winding and thence a spark is generated between both electrodes of the spark plug. [21] D_S prevents a pre-ignition event by the time IGBT is switched on and Z_S represents the impedance of the electrodes gap.

Currently, modern ignition coils, like the one used in this case, have been making use of microcontrollers for a wide range of functions, such as transmitting data regarding ignition parameters (e.g. charging current, spark duration, spark current or even information related to MultiCharge mode). [22] Furthermore, this control unit carries out diagnosis and measurement data acquisition which can be transmitted back to the ECU or be used for further operations inside the ignition coil. The microcontroller and respective circuitry that form the control unit are connected to the switch Q_1, represented in Figure 2.1. First and foremost, it was a purpose of the present work to develop a method to measure V_B through the microcontroller. The goal was to use the signals already collected by this component in order to minimize or eliminate the need to use additional electrical components. Within the scope of this aim, two solutions were brought up to discussion concerning the indirect measurement of breakdown voltage. Option A consisted of looking at collector voltage, V_{C-}, while Option B focused on the voltage across the capacitor that integrates the filter of the voltage across the secondary current sensor – a shunt resistor providing a voltage signal which is proportional to secondary current (hereinafter this voltage signal will be represented as V_{Is} for reasons of practicality). Figure 2.2 demonstrates the main functions of a microcontroller in an ignition PCB circuit as well as the nodes corresponding to Options A and B previously explained.
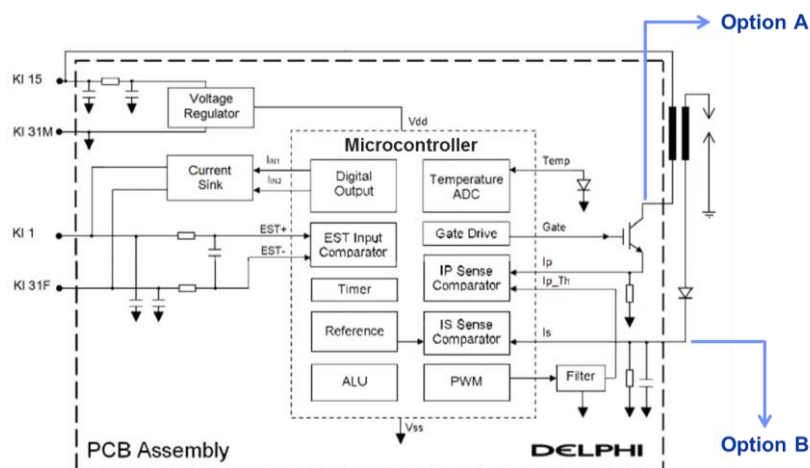

Figure 2.2. Ignition block diagram focusing on microcontroller-based PCB circuit and nodes where one can measure V_{C-} (Option A) and V_{Is} (Option B).

2.2 Direct Measurement of Breakdown Voltage

The first stage of this work comprised the direct measurement of breakdown voltage, along with other parameters related to the ignition coil. These tests aimed at understanding the effect of the breakdown event in the circuitry, as well as studying the influence of exterior factors (width of spark plug gap, pressure, engine load and fouling) in the set of parameters that are possible to obtain through the ignition coil electronics.
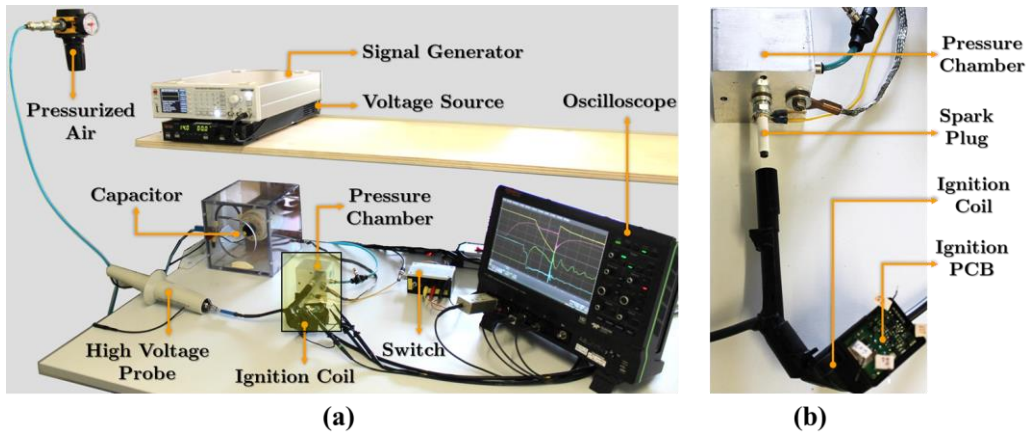
Figure 2.3. Laboratory setup for direct measurement of V_B: (a) complete assembly and (b) detail of the highlighted area of the image on the left.

All the signals were measured through the oscilloscope, the probes being connected to PCB components (resistors or capacitors), except for the high voltage probe which was directly connected to the high voltage end of the ignition coil. Each test essentially consisted in firing the spark plug under a set of conditions (explained next) and registering the corresponding waves and/or relevant values.

For these tests, the gap width was varied through two different methods: adjusting the electrodes gap with a pair of pliers until it was possible to measure the desired width in a microscope or adjusting the gap using a set of blades with different thicknesses. Although real-application values of the spark plugs gap are comprised between 700 μm and 950 μm, they had to be enlarged above this range (from 1000 μm to 2500 μm) in order to attain higher breakdown voltages in the laboratory (20 kV – 30 kV).

For the same reason, the pressure inside the combustion chamber was varied between 1 bar (atmospheric pressure) and 6 bar. Therefore, for the same spark plug gap, it was possible to obtain different V_B values.

The load capacitance was varied not only to obtain different V_B values but also to confirm the relation between the referred parameter and the observed slopes of different signals that were analyzed with the oscilloscope.

Brand new spark plugs were utilized as well as worn ones (after ca. 47800 km) to confirm the evolution of the breakdown voltage with the increasing wear of the plugs,

including not only gap growth but also fouled tips and modifications in the geometry and roughness of the electrodes surface. Throughout all the tests, the voltage source was providing 14 V (like the automobile battery when the vehicle is not running). Although during driving 20V are supplied instead of 14V, the voltage regulator contained in the ignition PCB provides only 5V to the rest of the circuit in all cases. For the referred tests, the signal generator was feeding a square signal with amplitude and frequency equal to 5 V and 10 Hz, respectively.

2.3 Indirect Measurement of Breakdown Voltage

The following stage of this work was focused on the breakdown voltage detection through an indirect method. Therefore, a setup similar to the first one was used, except for the fact that the oscilloscope was replaced by a laptop. The latter was connected to the PCB circuit not by probes but instead by a cable inserted in the PCB software pins. Data was collected from the microcontroller located in the PCB.
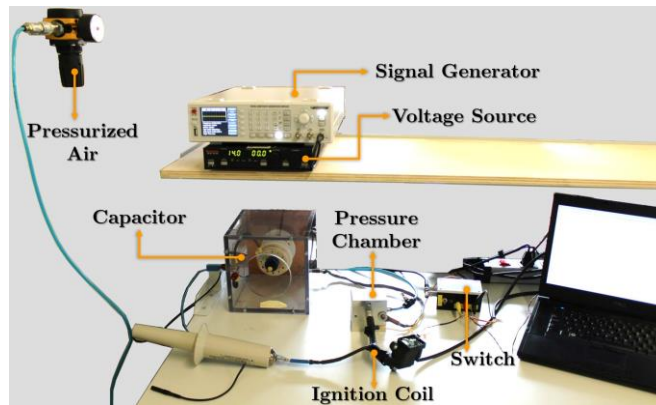
Figure 2.4. Laboratory setup for indirect measurement of V_B.

A terminal software was used as an interface to collect data in the laptop and transfer it to an Excel worksheet for further analysis.

For preliminary tests in the car, an oscilloscope was connected to one of the four ignition coils mounted in the engine, to confirm the signals observed in laboratory environment. Once these were assured, the aforementioned software was also used in the car tests. In this case, the laptop was connected through a cable to the ignition coil mounted in the engine, the same way it is presented in Figure 2.4.

3 Results and Discussion

3.1 Paschen Law

For all the laboratory measurements, pressure chamber was chosen to be fed with air, instead of pure nitrogen, in order to simulate the real conditions, including the formation of ozone during combustion which might influence V_B. The theoretical calculations based on Paschen Law for air allowed the plot in Figure 3.1 to be drawn. For those, it was considered $A = 11,25 \text{ cm}^{-1}.\text{Pa}^{-1}$ and $B = 273,77 \text{ V}.\text{cm}^{-1}.\text{Pa}^{-1}$.
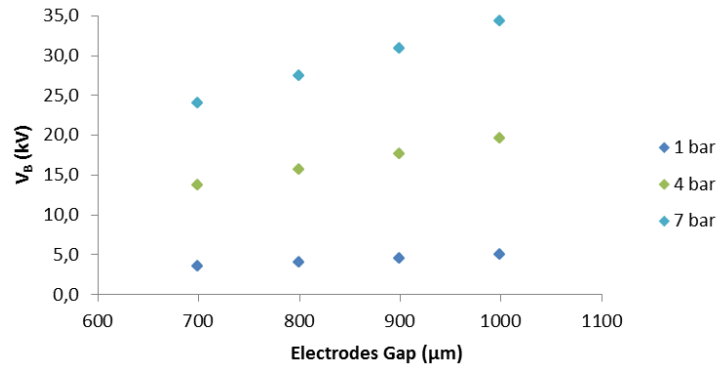
Figure 3.1: Theoretical values of V_B vs. electrodes gap for 1 bar, 4 bar and 7 bar.

However, it was not possible to obtain the predicted values. As instead, V_B values were consistently lower than the theoretical ones (as one can notice form the difference in V_B axis from Figure 3.1 to Figure 3.2). Only three gap sizes were used for this test since the process of customizing this feature was time-consuming. The results presented in Figure 3.2 were obtained from the average of 15000 sweeps.
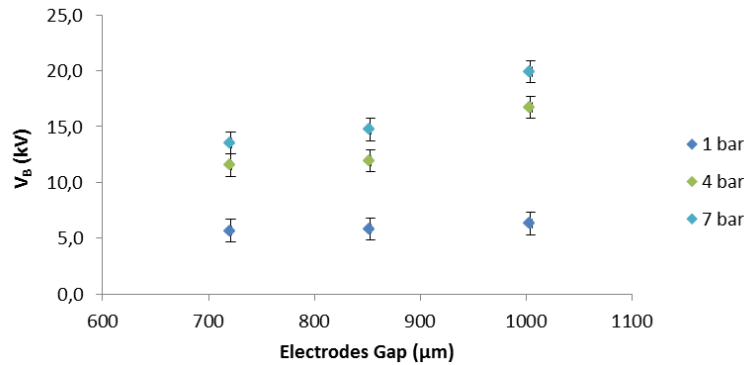
Figure 3.2: Experimental values of V_B vs. electrodes gap for 1bar, 4 bar and 7 bar.

In order to obtain breakdown voltage values above 30 kV, the gap was widened between 2000 μm and 2500 μm (approximately the double of what was predicted by the theoretical calculations). It was necessary to obtain this magnitude of V_B because that is the voltage range created by a wider gap which can be found in worn spark plugs.

3.2 Spark Plug Wear

In total, twelve spark plugs were submitted to the tests, of which six were brand new and the other six had already been used in the car. Four out of these last six spark plugs were used for ca. 47800 km. Figure 3.3 allows the distinction between new and worn electrodes. In the image on the right, a set of wear phenomena can be identified: gap growth, increased roughness of the electrodes surface, changes in the electrodes geometry and a darker color surrounding the electrodes that indicates fouling.
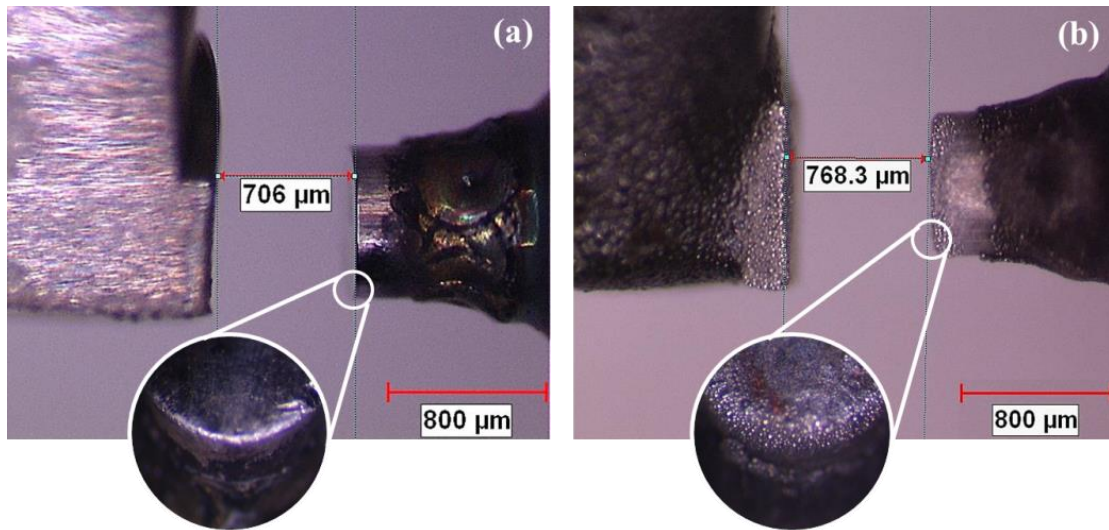
Figure 3.3: Comparison between (a) new spark plug electrodes and (b) worn spark plug electrodes after 47800 km.

Figure 3.4 is enlightening about the relation between spark plugs wear and the increase of breakdown voltage. It shows the results of preliminary tests which aimed to distinguish a new plug from a worn one through V_B (an extra capacitor was added to the setup used in the laboratory, representing load capacitance, C_{Load}).
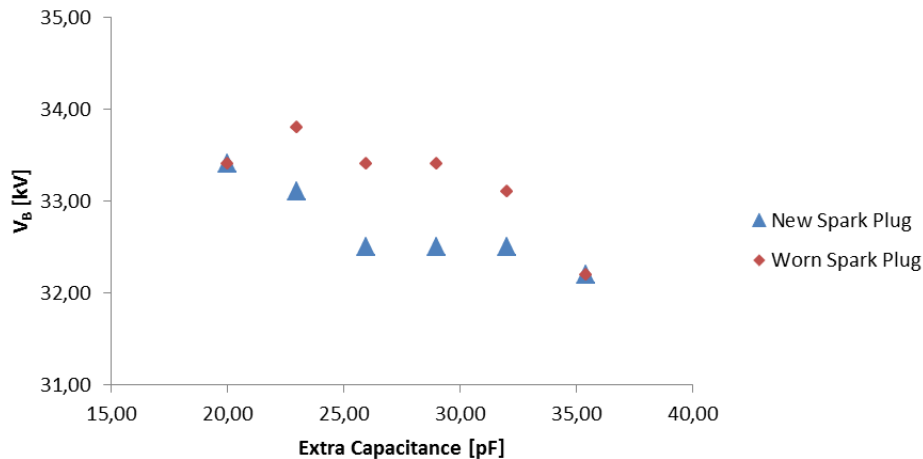
Figure 3.4. Breakdown voltage as a function of capacitance for a new and a worn spark plug.

Firstly, Figure 3.4 shows that the breakdown voltage diminishes with the increase of load capacitance. In addition, although a correlation between V_B and wear conditions can not yet be quantified, it is clear that the latter affects the first one in the way it was expected, *i.e.* even for the same pressure and spark plug gap combination, a worn spark plug presents a higher voltage.

3.3 Selection of Parameters

Previous tests carried out in Delphi showed that collector voltage could represent a suitable parameter for indirect breakdown voltage detection; hence it was one of the premises for this work. In addition, it was also noticed a correlation between V_B and the duration of the ignition event. These originated Options A and B referred in Section 2.1. Tests in the wake of this study shown that the voltage across the secondary current shunt resistor (secondary current sensor) in the moment V_B attains its maximum value is a reliable parameter as well. However, it is not possible to implement that option in the existing microcontroller, fact that will be further explained once the oscilloscope curves are disclosed.

The aforementioned signals are simultaneously presented in Figure 3.5. For higher breakdown voltages, the secondary voltage rise time is longer and, for that reason, all the signal lengths are extended, have not been detected any change in the curves course (assuming load capacitance is kept constant).

Figure 3.5. Secondary voltage (yellow), V_C (red), IGBT gate voltage (blue) and V_{Is} (green) during breakdown event, for V_B=27 kV and C_{Load}=30 pF.

Yellow curve demonstrates how the voltage in the high voltage side of the secondary winding rises until the breakdown phenomenon takes place. This voltage is in fact positive, unlike what is showed in Figure 3.5, which means that V_B is the highest secondary voltage attained immediately before the breakdown (altho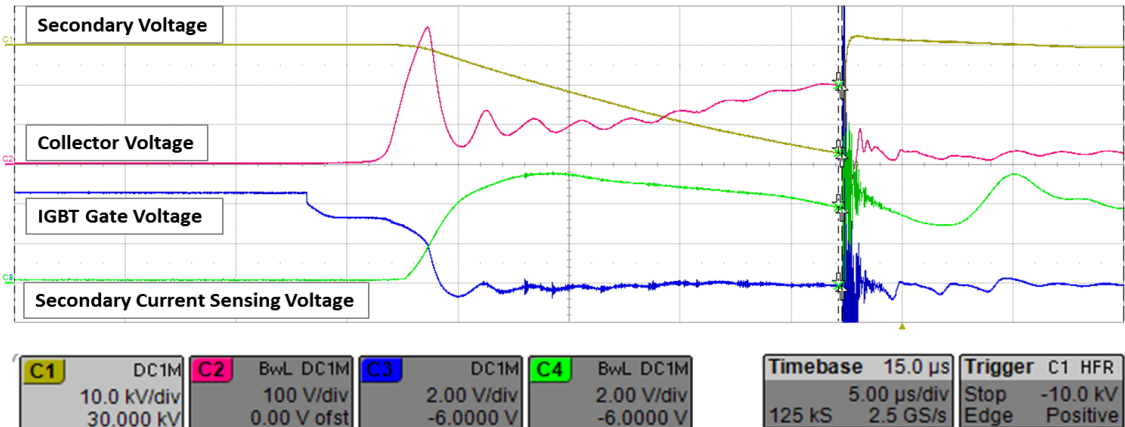ugh it is the minimum of the yellow curve). The voltage in the collector of the IGBT – red curve – is the reflection of the first one. Therefore, the last point of the collector voltage before the breakdown is directly proportional to the breakdown voltage. IGBT gate signal was collected solely as a reference, since its step exhibits the instant when primary winding of the ignition transformer is disconnected from ground, thus transferring the energy to the secondary winding to initiate the discharge. Secondary current sensing voltage was considered to be equal to zero until the breakdown, when the primary winding would transfer its energy to the secondary winding. However, because the green curve shows a great amplification of this specific moment, one can see that this energy transference starts a few microseconds earlier, allowing for the secondary voltage to start building up until it is sufficient to ignite the fuel molecules in the air/fuel mixture.

It is important to notice that the noise of the green and blue curves is only picked up by the external measurement equipment (oscilloscope) and not visible for the coil integrated microcontroller. Therefore, it is not possible to trigger with the microcontroller software since a steep slope is needed. Even by using a second signal as a breakdown timing trigger and measuring the V_{Is} in that instant, the delay between the first one and the second one leads to a V_{Is} value which is measured out of the specified time range. Thereby this is not considered a suitable option.

There were performed two tests which included all the twelve spark plugs with no distinction concerning wear conditions: to assess the relation between V_B and V_C

(Figure 3.6) and the relation of V_B with the time between the IGBT turning off and the moment when V_B achieves its maximum value (Figure 3.7).
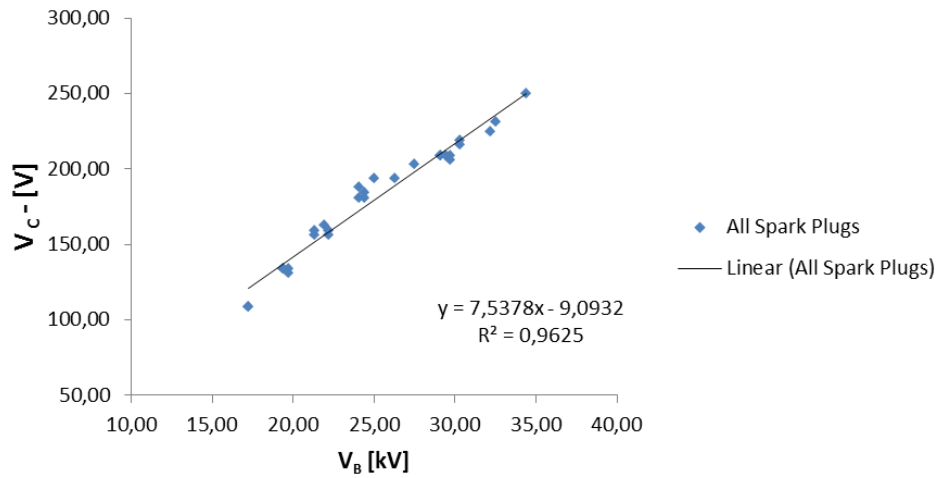
Figure 3.6. Collector voltage vs. breakdown voltage (Option A), neglecting differences in wear conditions of the spark plugs.
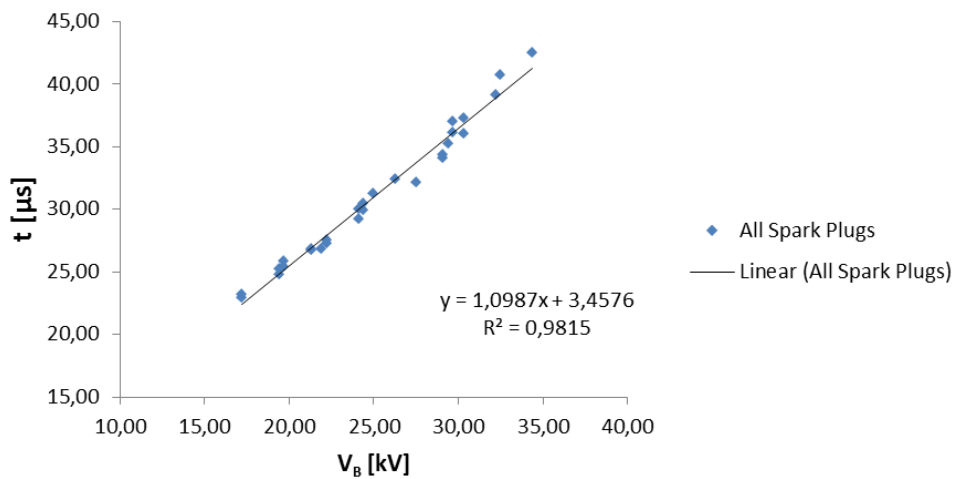
Figure 3.7. Time between IGBT turning off and V_B peak vs. breakdown voltage (Option B), neglecting differences in wear conditions of the spark plugs.

Although both parameters show a significant relation with the breakdown voltage, it would be ideal that the capacitance could not affect that relation. That way, changes in load capacitance during driving would not change the measurements, considering every other factors constant (*e.g.* environmental conditions, speed, etc). In addition, it is also known that C_{Load} influences V_B even if pressure and spark plug gap are kept constant.
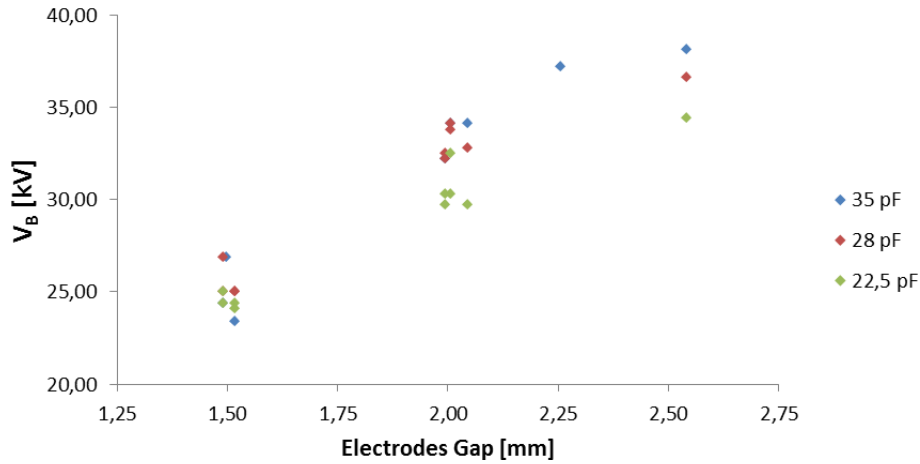
Figure 3.8. Breakdown voltage vs. electrodes gap for different load capacitances (p = 7 bar).

One can observe in Figure 3.8 that, in general, for the same spark plug gap (which, in this study, is associated with similar wear conditions) the breakdown voltage increases with load capacitance.

The next test, which consisted in varying C_{Load} for Options A and B, provided the results presented in Figure 3.9 and Figure 3.10.
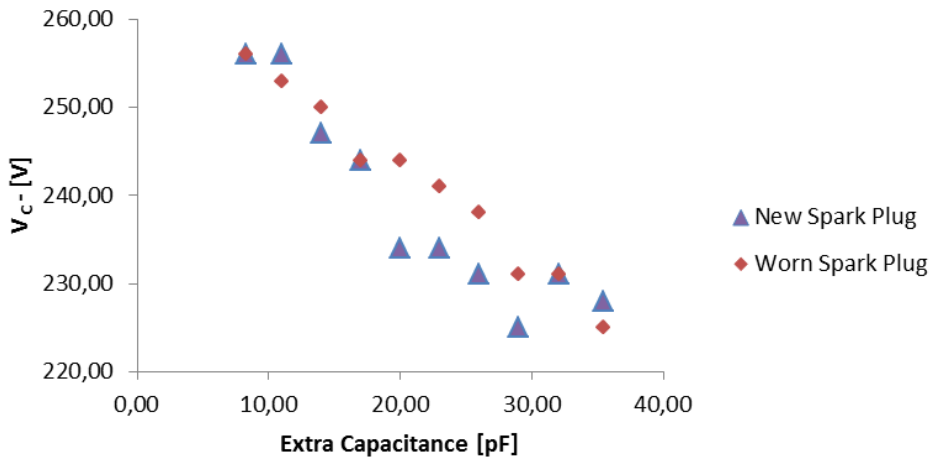
Figure 3.9. Collector voltage vs. extra load capacitance (Option A), for new and worn spark plugs.

Although, generally, an increase of the load capacitance implies a lower break-down voltage (Figure 3.4) and therefore a lower collector voltage (Figure 3.6), some of the consecutive measurements that are plotted in Figure 3.9 have the V_B value in common, and yet the collector voltage diminishes with C_{Load} which excludes V_C - as a capacitance-independent variable.

16
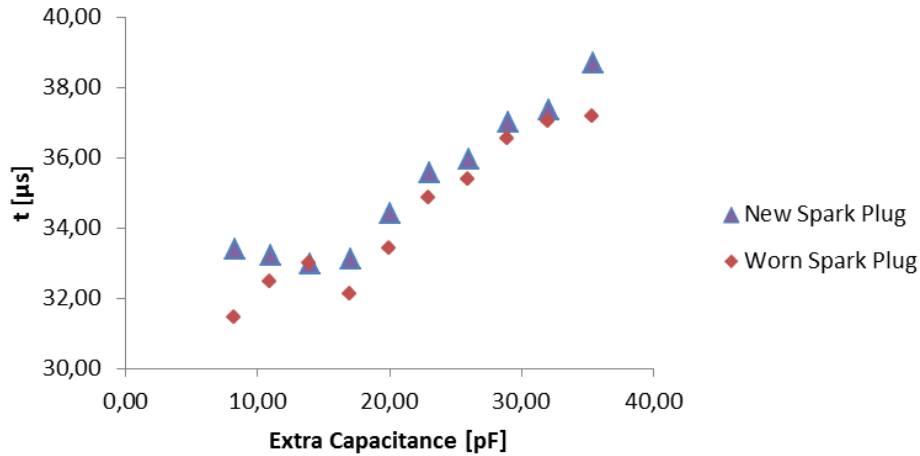
Figure 3.10. Time between IGBT turning off and V_B peak vs. extra load capacitance (Option B), for new and worn spark plugs.

With a similar interpretation of Figure 3.9, Figure 3.10 also shows that the measured time interval is not independent from the capacitance (once again, even when comparing measurements with the same breakdown voltage value).

To complement the information obtained from Figure 3.9 and Figure 3.10, Appendix A shows the collected data during the referred test, highlighting four different groups characterized by common breakdown voltage and wear conditions, in which one can observe that collector voltage and the chosen time interval respectively decreases and increases with the increase of load capacitance.

Table 3.1 allows for a decision between Options A and B based on a practical point of view concerning not only the simplicity and reliability of the process but also the associated costs to the respective implementation.

Table 3.1. Comparison of the implementation requirements for Options A and B.

	Option A	Option B
Measured variable	Collector voltage	Secondary current
Implementation	• Sample and hold circuit • D/A converter	• Software modification • I_S sensing circuit (if not already present)
Implementation cost	Development and additional components cost	Development cost
Measured variable depend on	• Pressure at the spark gap • Load capacitance	• Pressure at the spark gap • Load capacitance
Breakdown timing detection	Available	Not available

Since the present work was developed based on a MultiCharge ignition coil, which comprises a shunt resistor to measure I_S and respective filter, for Option B alone,

no hardware modifications need to be undertaken. Option B entails exclusively a software modification, representing the lowest cost option. Therefore, it is preferred, as long as reliability requirements are fulfilled. Those requirements must mainly represent a goal for the tests in the car which bring about a set of incontrollable conditions. Although the individual cost of the components demanded in Option A is not significant, it is a significant issue when considering mass production.

V_{Is} does not allow for the exact breakdown timing identification, i.e. the respective curve does not have a steep slope by the time secondary voltage gets to its maximum value (minimum of the respective curve). However, this does not necessarily represent an obstacle for the implementation, according to further tests, which considered a filtered EST (electronic spark timing) voltage signal to seek for that reference breakdown timing. The aforementioned tests were performed to determine the interrelationship between load capacitance, breakdown voltage and the following coil parameters: V_{Is}, IGBT gate voltage and filtered EST voltage.

Figure 3.11 to Figure 3.13 demonstrate how the following timings vary with V_B and C_{Load} ($C_{Load} = 35$ pF $\vee$ $C_{Load} = 15$ pF since those were the maximum and minimum capacitances provided by the extra capacitor used in both laboratory tests setups):

- t_B: always positioned at the breakdown instant, this signal can serve as a reference and is detected every time the filtered EST voltage drops below a pre-determined trigger (2.5 V in this case);
- t_{IGBT}: start trigger for all the measurements since it is internally generated;
- t_{Is}: moment when I_S drops below the threshold $V_{th}(I_S)$; $V_{th}(I_S)$ is predefined according to the breakdown voltage value that one considers critical (for greater critical breakdown voltages, a lower threshold must be selected).
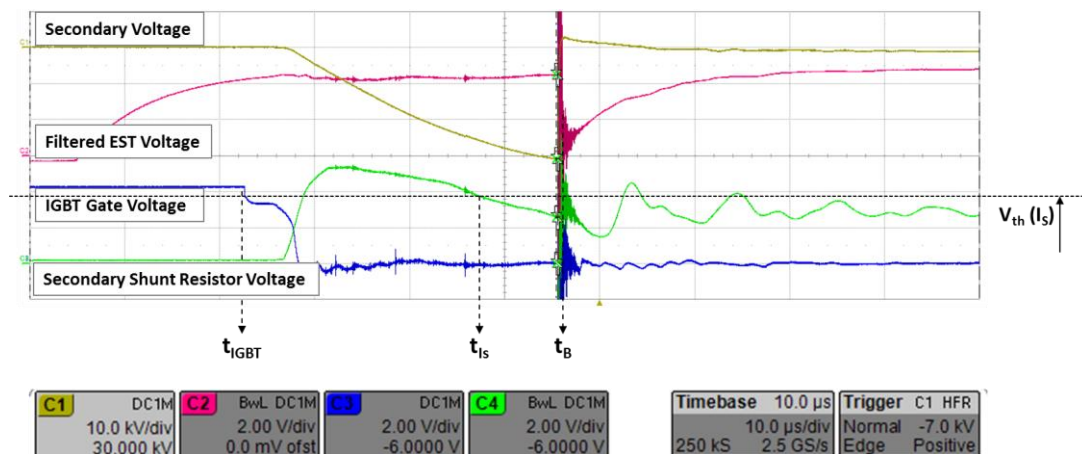
Figure 3.11. Secondary voltage (yellow), filtered EST voltage (red), IGBT gate voltage (blue) and V_{Is} (green) during breakdown event, for $V_B = 31$ kV and $C_{Load} = 35$ pF.
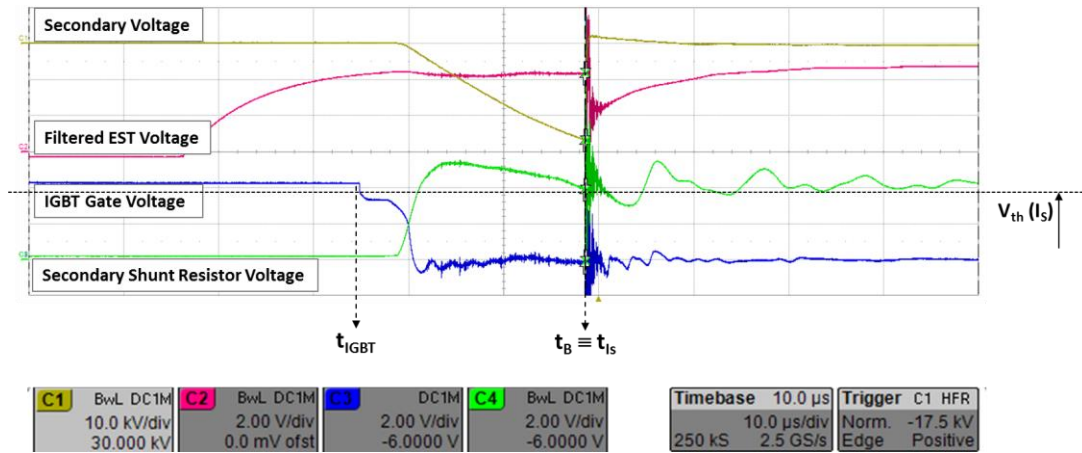
Figure 3.12. Secondary voltage (yellow), filtered EST voltage (red), IGBT gate voltage (blue) and V_{Is} (green) during breakdown event, for $V_B = 27$ kV and $C_{Load} = 35$ pF.
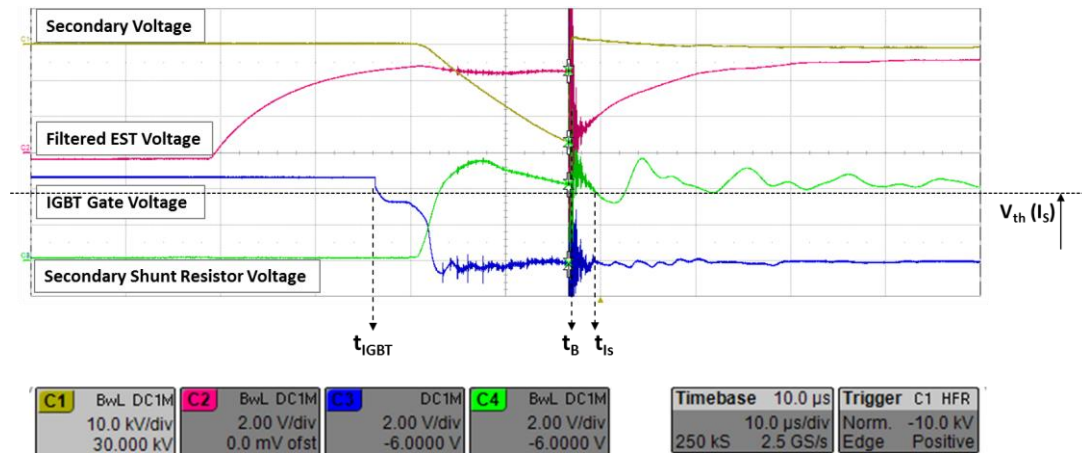
Figure 3.13. Secondary voltage (yellow), filtered EST voltage (red), IGBT gate voltage (blue) and V_{Is} (green) during breakdown event, for $V_B = 27$ kV and $C_{Load} = 15$ pF.

It can be observed that the time intervals t_B - t_{IGBT} and t_{Is} - t_{IGBT} increase with C_{Load} and V_B, although the latter has a much greater influence on such parameter, as it was expected. It is also shown that the amplitude of the filtered EST voltage peak increases with V_B and decreases with C_{Load}. This signal was expected to be a constant line in this discharge phase. However, the electrical components that filter the EST signal before it is fed into the microcontroller create an "antenna" effect that increases the amplitude of the noise originated in the high voltage end of the secondary winding. As a result, filtered EST signal serves as a detector circuit for the exact breakdown timing. It should be noticed that the existence of this filtered EST voltage peak was confirmed not only in laboratory conditions but also in real driving conditions.

3.4 Implementation of the Modified Software in the Micro-controller

This work called for a modification in the current software of the microcontroller. Since it is an 8-bit microcontroller, the chosen monitoring method could not be too complex or occupy too much memory.

For that reason, it was chosen for the microcontroller not to measure both V_{Is} and filtered EST voltage. As instead, the microcontroller just has to collect the information about the first event to occur – either t_{Is} or t_B. Whenever the microcontroller is performing the measurements, it is considered $t_{IGBT} = 0$ (moment when the microcontroller starts the measurement), therefore t_B and t_{Is} represent the interval since the IGBT turns to off-state until the respective event takes place. t_{OUT} represents the maximum timing for which the microcontroller seeks for the predetermined conditions.

To make sense of the results, one defines $V_{B,crit}$ as the voltage that represents a critical state of electrodes wear and three main conditions should be established regarding a primary condition: $t_{Is}, t_B \in [0; t_{OUT}]$.

1. $t_{Is} > t_B \ \lor V_{Is} > V_{th}(I_S) \ \forall \, t \in [0; t_{OUT}] \Rightarrow V_B < V_{B,crit}$
2. $t_{Is} = t_B \ \Rightarrow V_B = V_{B,crit}$
3. $t_{Is} < t_B \Rightarrow V_B > V_{B,crit}$

For the present work, it was used the only comparator available to set the trigger for $t_{Is} - V_{th}(I_S)$ – whereas the trigger for t_B was set through a reference value already existing in the microcontroller hardware. Once the microcontroller continuously transmits to the ECU one of the previous conditions per each cycle, ECU should be able to, under statistical data processing, determine whether the spark plug is undertaking critical breakdown voltage conditions (*i.e.* the third condition is obtained in hundreds of almost consecutive measurements). This data analysis is performed while the ECU possesses real-time information concerning speed, load and rotations per minute (rpm). That is the major advantage in the collaboration between ignition system and the ECU instead of performing the whole process coil-internally. It should be noticed that a single measurement does not allow for any reliable conclusion, particularly regarding the unfavourable set of conditions that the ignition system undergoes in the car (lack of clean environment, inconsistent speed, load, pressure, temperature and fuel quality, and the like).

3.4.1 Car Tests

There were performed tests in the car to assess the applicability of the foregoing method. The tests consisted in measuring the previously referred timings while the car

was driven along a closed circuit (Figure 3.14). Speed and load values were registered in specific points of the circuit.
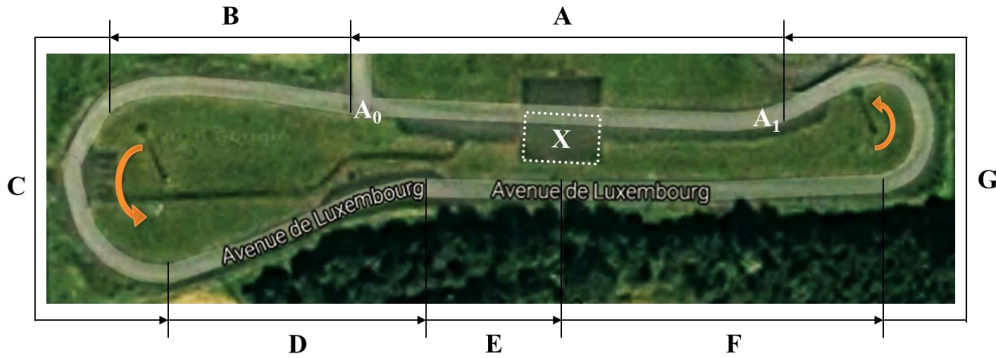

Figure 3.14. Closed circuit to the car test where A, C, E, F and G are flat surfaces while B is a downhill and D is an uphill (considering the direction of the arrows); X is a stopping area.

Since, for normal driving conditions, breakdown voltage is maintained below 20 kV, it was not possible to measure t_B because the respective voltage peak was too small. In order to detect it, the microcontroller used would need an additional comparator to create a different trigger for this signal. Even so, tests were performed to confirm whether t_{Is} could be sufficient *per se*.

It is highlighted a part of the software results in which the car was braking from A_1 to A_0, stopping therein. Once stopped (without turning off the engine) the driver accelerated towards A_1 in reverse gear and then kept the speed constant. Once the car stopped at A_1, it accelerated again, in first gear, towards A_0. The foregoing description corresponds to Appendix B. This segment is representative of the whole circuit and it was chosen as an example due to the frequency of load and speed variation throughout.

It is possible to observe that high speed and load conditions always present the same value of t_{Is} (13.5 µs). The same way, every time the car runs under low speed and load conditions, the t_{Is} is 14.5 µs. Zeros in the second column indicate the moments when the car was stopped or under speed and load conditions near zero. Since the car test were performed with suitable spark plugs (not worn out), the breakdown voltage did not attain values between 30 kV and 40 kV, which the method described in section 3.4. was designed to detect. Therefore, the peak of the filtered EST signal was not sufficient for the software to detect it, reason why all the values in the first column of Appendix B are equal to zero. Finally, in the last column, zeros indicate that none of the measures got to t_{OUT}, i.e. the microcontroller detected at least one variable before the maximum time it is able to proceed with the measurements.

Theoretically, establishing the relation between t_{Is} and speed/load conditions, since all this information is already present in the automobile, it is possible to detect when the breakdown voltage is higher than the desirable value, because the values de-

scribed above would increase. However, in the last part of the tests, the values were no longer the same which was later explained by the fact that the voltage regulator in the ignition PCB was not working properly, originating an offset in all the signals. Although this is the kind of situation one can detect in experimental conditions, the same issue would not be detected in the real application and the ECU would take the wrong conclusions, possibly alerting for a problem that would not exist. To prevent that, the filtered EST voltage peak must be detected, since the offset would not change the relation between t_B and t_{Is}.

4   Conclusion and Future Perspectives

During this master thesis it was possible to study not only the ignition coil integrated system but also – obviously with significantly less detail – the engine, and surrounding components, and the ECU. This, in turn, allows for a better understanding of what the solution might comprise and what limitations one has to consider. In addition to this, the implementation of the solution in mass production must play a role on the decision as well. For example, the software modification that is suggested by this work eliminates the need for a spark plug wear sensor (which would imply the replacement of the current spark plugs for different ones that may not be as optimized as the first ones); at the same time, it eliminates the need to add circuitry to the ignition coil which would increase the cost of those parts in mass production. This way, a customer-driven solution is accomplished, not entailing significant design and cost changes.

For the purpose of the laboratory experiments, the most relevant variables consisted in the spark plug gap (associated with wear conditions, although without quantification of such relation for now), pressure inside the combustion chamber and load capacitance. For different combinations of the aforementioned parameters, it was shown that a secondary current sensing circuit may also serve as a breakdown voltage sensor, presenting reliable results for different values of breakdown voltage and load capacitance. Still, the most challenging hurdle consists in isolating the gap enlargement from other events that also contribute to an increase of the breakdown voltage, such as engine load and speed, spark plug fouling and pressure and temperature in the electrodes gap.

Further car tests aim to overcome this, since the real driving conditions are not possible to be reproduced in the laboratory. Once reliable results are obtained, a correlation between these and the spark plug wear must be quantified. From the low amount of car tests that was performed in the wake of this thesis, one has the option of coming up with a statistical data analysis that include but is not limited to the three main conditions referred in Section 3.4 in order to eliminate the need for t_B measurement. Alternatively, this solution might just be implemented on ignition coils which microcontroller provides two available comparators in order to create an additional trigger for the filtered EST voltage signal and then obtain t_B. Although this work did not achieve a solid and finished solution, it opened doors for researches with high interest in short term, regarding Horizon 2020 and the trend for a smart, connected and green technology.

References

[1]   E. Commission, "Executive Summary of the Impact Assessement Accompanying the Communication from the Commission 'Horizon 2020 - The Framework Programme for Research and Innovation,'" Brussels, Belgium, 2011.

[2]   *Setting Emission Performance Standards for New Passenger Cars as part of the Community's Integrated Approach to Reduce CO2 Emissions from Light-duty Vehicles*. European Parliament and Council of the European Union: Official Journal of the European Union, 2009.

[3]   B. Geringer, "Demands on Gasoline Engines with Focus on the stringent Fuel Economy and Emission Limits until 2020," in *Advanced Ignition Systems for Gasoline Engines*, 2013, pp. 1–17.

[4]   P. Weyand, F. Lorenz, S. Schilling, and D. P. Systems, "Adaptive Continuous Spark Ignition as Enabler for High Dilution EGR Operation," in *2nd IAV Advanced Ignition Conference*, 2014.

[5]   S. Javan, S. V. Hosseini, S. S. Alaviyoun, and F. Ommi, "Effect of electrode erosion on the required ignition voltage of spark plug in CNG spark ignition engine," *J. Engine Res.*, vol. 26, no. Spring 2012, pp. 31–39, 2013.

[6]   T. Yoshinaga, T. Igashira, K. Mori, H. Kawai, and S. Morino, "Ignition System for Internal Combustion Engines," US 4,350,137, 1982.

[7]   F. Lorenz, P. Weyand, E. Jacque, and S. Schilling, "Advanced Ignition Systems: Technical Possibilities and Limitations," in *SIA Conference The Spark Ignition Engine of the Future*, 2013.

[8]   R. Maly, "Spark Ignition: Its Physics and Effect on the Internal Combustion Process," in *Fuel Economy in Road Vehicles Powered by Spark Ignition Engines*, J. C. Hilliard and G. S. Springer, Eds. New York, USA: Springer Science+Business Media, 1984.

[9]   G. Bayard, "Functional Aspects of conventional Spark Ignition for Internal Combustion Engines," in *Advanced Ignition Systems for Gasoline Engines*, 2013, pp. 180–190.

[10]   V. Ganesan, *IC Engines*, 4th Ed. New Delhi: Tata McGraw Hill Education Private Limited, 2012.

[11]   W. L. Hosch, "Nikolaus August Otto," *Encyclopædia Britannica*. 2006.

[12]   H. N. Gupta, *Fundamentals of Internal Combustion Engines*, 2nd ed. New Delhi, India: PHI Learning Pvt. Ltd., 2006.

[13]   "GP Customs." [Online]. Available: http://www.gpcustoms.com/images/ZK_Grafik_Aufbau_10.gif. [Accessed: 27-Aug-2016].

[14]   K. Nishio, S. Takagi, and Y. Suzuki, "Spark Plug and Manufacturing Process Thereof," US 4,414,483, 1983.

[15]   S. Javan, S. V. Hosseini, and S. S. Alaviyoun, "An Experimental Investigation of Spark Plug Temperature in Bi-Fuel Engine and Its Effect on Electrode

Erosion.pdf," *Int. J. Automot. Eng.*, vol. 2, no. 1, 2012.

[16]   F. Lorenz, "Untersuchung und Entwicklung von MultiCharge-Zündsystemen für direkteinspritzende Ottomotoren," Fachhochschule Aachen, 2009.

[17]   F. Paschen, "Ueber die zum Funkenübergang in Luft, Wasserstoff und Kohlensäure bei verschiedenen Drucken erforderliche Potentialdifferenz," *Ann. Phys.*, vol. 273, no. 5, pp. 69–96, 1889.

[18]   K. Burm, "Calculation of the Townsend Discharge Coefficients and the Paschen Curve Coefficients," *Contrib. Plasma Phys.*, vol. 47, no. 3, pp. 177–182, 2007.

[19]   F. Löffler and C. Siewert, "Homogeneous coatings inside cylinders," *Surf. Coatings Technol.*, vol. 177–178, pp. 355–359, 2004.

[20]   A. J. Wallash and L. Levit, "Electrical breakdown and ESD phenomena for devices with nanometer-to-micron gaps," *Proc. SPIE*, vol. 4980, pp. 87–96, 2003.

[21]   J. W. Boyer, R. O. Butler Jr, and D. J. O'Connor, "Multicharge Ignition System having Secondary Current Feedback to Trigger Start of Recharge Event," US 6,378,513 B1, 2002.

[22]   S.-M. Eisen, S. Bolz, H. Schmauss, A. Reuther, and M. Goetzenberger, "Ignition Device for an Internal Combustion Engine and Method for Operating an Ignition Device for an Ignition Device for an Internal Combustion Engine," US 2013/0263835 A1, 2013.
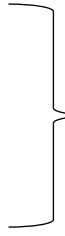
Appendix

Appendix A. Result of the test to assess the correlation between C_{Load} and V_C - (Figure 3.9) and C_{Load} and t_{Is} - t_{IGBT} (Figure 3.10).

Spark Plug	Extra Cap. [pF]	V_B [kV]	V_C - [V]	t_{Is} - t_{IGBT} [µs]
New	8,28	35,30	256,00	33,38
	10,96	35,60	256,00	33,21
	13,99	34,70	247,00	32,97
	17,02	33,40	244,00	33,10
	20,00	33,40	234,00	34,40
	23,01	33,10	234,00	35,56
	25,97	32,50	231,00	35,97
	29,01	32,50	225,00	37,00
	32,02	32,50	231,00	37,35
	35,43	32,20	228,00	38,68
Worn	8,28	34,70	256,00	31,43
	10,96	35,30	253,00	32,46
	13,99	34,70	250,00	32,96
	17,02	33,40	244,00	32,10
	20,00	33,40	244,00	33,40
	23,01	33,80	241,00	34,85
	25,97	33,40	238,00	35,35
	29,01	33,40	231,00	36,53
	32,02	33,10	231,00	36,99
	35,43	32,20	225,00	37,16

Note: each color represents a group of data with the same breakdown voltage and wear conditions.

Appendix B. Segment of the results from the car tests.

t_B [μs]	t_{Is} [μs]	t_{OUT} [μs]		
0	14,5	0	·····	A
0	14,5	0		
0	14,5	0		
0	14,5	0		
0	14,5	0		Braking
0	14,5	0		
0	14,5	0		
0	14,5	0	·····	A_0
0	13,5	0		
0	13,5	0		
0	13,5	0		Starting in
0	13,5	0		Reverse Gear
0	13,5	0		
0	14,5	0		
0	1	0		
0	0	0		
0	61,25	0		
0	0	0		
0	14,5	0		
0	0	0		
0	0	0		Reverse
0	0	0		Gear
0	13,5	0		
0	0	0		
0	14,5	0		
0	0	0		
0	0	0		
0	14,5	0		
0	14,5	0		
0	13,5	0		Braking
0	0	0		
0	13,5	0		
0	0	0	·····	A_1
0	13,5	0		
0	13,5	0		
0	13,5	0		Accelerating
0	13,5	0		
0	14,5	0		
0	13,5	0	·····	A